it appears possible that the inclusion of triple products of hydrodynamic variables in our formalism converts η_0 into a dressed η.

ACKNOWLEDGMENTS

The authors gratefully acknowledge the vigilance of Ira Michaels in locating their careless errors. We would also like to thank the NATO Research Grants Programme for the opportunity of discussing this problem with Professor P. Mazur and Dr. D. Bedeaux at the University of Leiden.

*Work supported in part by a grant from the National Science Foundation.
†National Science Foundation Postdoctoral Fellow.
[1]G. Stokes, Trans. Camb. Philos. Soc. **9**, 5 (1856).
[2]A. Einstein, *Investigations on the Theory of Brownian Movement*, edited by R. Fürth (Dover, New York, 1956).
[3]P. V. Cheng and H. K. Schachman, J. Polym. Sci. **16**, 19 (1955).
[4]John T. Edwards, J. Chem. Educ. **47**, 261 (1970).
[5]Myong-Ku Ahn, S. J. Knak Jensen, and Daniel Kivelson, J. Chem. Phys. **58**, 428 (1973); Stuart A. Rice and John G. Kirkwood, J. Chem. Phys. **31**, 901 (1959).
[6]H. Mori, Prog. Theor. Phys. **33**, 423 (1965).
[7]R. Zwanzig, Phys. Rev. **124**, 983 (1961).
[8]B. U. Felderhof and I. Oppenheim, Physica (Utr.) **31**, 1441 (1965).
[9]B. J. Alder and T. E. Wainright, Phys. Rev. A **1**, 18 (1970).
[10]T. Keyes and Irwin Oppenheim, Phys. Rev. A **7**, 1384 (1973).
[11]K. Kawasaki, Ann. Phys. (N.Y.) **61**, 1 (1970).
[12]M. H. Ernst, E. H. Hague, and J. M. J. van Leeuwen, Phys. Rev. Lett. **25**, 1254 (1970); Arkiv Fys.-Trondheim **8** (1971); J. R. Dorfman and E. G. D. Cohen, Phys. Rev. Lett. **25**, 1257 (1970); T. E. Wainright, B. J. Alder, and D. M. Gass, Phys. Rev. A **4**, 233 (1971).
[13]H. Lamb, *Hydrodynamics* (Cambridge U.P., Cambridge, England, 1932).
[14]Y. Pomeau, Phys. Rev. A **5**, 2569 (1972); M. H. Ernst and J. R. Dorfman, Physica (Utr.) **61**, 157 (1972).
[15]Allan Widom, Phys. Rev. A **3**, 1394 (1971).
[16]T. E. Wainright, B. J. Alder, and D. M. Gass, Phys. Rev. A **4**, 233 (1971); Robert Zwanzig, in *Proceedings of the Sixth IUPAC Conference on Statistical Mechanics*, edited by Stuart A. Rice, Karl F. Freed, and John C. Light (University of Chicago Press, Chicago, 1972).

PHYSICAL REVIEW A VOLUME 8, NUMBER 2 AUGUST 1973

t-Matrix Calculations of the Ground-State Energies of Solid He^3 and Solid H_2

V. Canuto* and J. Lodenquai†
Institute for Space Studies, Goddard Space Flight Center, National Aeronautics and Space Administration, New York

S. M. Chitre‡
Institute for Space Studies, Goddard Space Flight Center, National Aeronautics and Space Administration, New York, Belfer Graduate School of Science, Yeshiva University, New York

(Received 22 March 1973)

The ground-state energies of solid He^3 and H_2 at various densities are calculated using a self-consistent method in the t-matrix formulation. The two-body equation of motion is solved by expanding the two-body wave function in terms of partial waves. The partial-wave expansion gives rise to a set of coupled differential equations which are solved numerically for the ground-state eigenfunctions. The calculations for He^3 are done using three different two-body potentials, the Lennard-Jones potential, the Beck potential, and the Frost-Musulin potential. The calculations for H_2 are done using the Mason-Rice two-body potential. A bcc structure is assumed for solid He^3, while an fcc structure is assumed for solid H_2. Exchange effects are neglected. Figures and tables are given which compare the present results with those of other authors.

I. INTRODUCTION

The ground-state properties of solid helium, which is well known to be the most characteristic quantum crystal, have been the subject of quite intensive theoretical and experimental activities in recent years. There exist a number of excellent expositions dealing with the behavior of solid He^3 among which one may mention the papers of Werthamer[1] and Guyer.[2] Here one can find a series of convincing arguments and figures exhibiting the rather unique character of He isotopes when compared with other solid rare-gas elements such as Ar, Ne, etc. The helium solid is more "quantum" than solid H_2 or D_2 even though the masses of the molecules of the latter solids are smaller than that of He, the kinetic energies larger, and consequently the excursions around

the lattice sites more pronounced. The potential energy comes to the rescue in all cases except that of He isotopes, where the potential turns out to be the least attractive among all rare gases. As a consequence of this rather peculiar state of affairs, classical lattice dynamics breaks down rather badly and a quantum many-body treatment is therefore needed to describe the system.

The problem of quantum crystals has been studied by a variety of methods. A method was suggested by Nosanow,[3] who employed the cluster-expansion technique introduced by Van Kampen[4] by expressing the trial wave function as a product of single-particle Gaussian wave functions and a short-range correlation. Recently, Hansen and Pollack[5] adopted the variational calculation to compute the ground-state energies of solid He^3 and He^4 by a Monte Carlo method and improved considerably upon the original results.

Among the various many-body techniques used to study the properties of solid He, the t-matrix method has received renewed attention due to the works of Sarkissian,[6] Guyer and Zane,[7] and Brandow.[8] The Bethe-Goldstone equation for the two-body wave function $\psi_{12}(\vec{r})$, in the form introduced by Iwamoto and Namaizawa,[9] has been studied more recently by Sarkissian[6] and Guyer and Zane,[7] who, however, did not perform an angular momentum expansion of the wave function. Such an analysis is performed in this work. The first explicit angular momentum expansion of $\psi_{12}(\vec{r})$ was performed, to our knowledge, in a paper by Brueckner and Frohberg,[10] where the authors showed that high partial waves up to $l \geq 6$ are needed for a sensible convergence.

In this paper we determine the ground-state energies of solid He^3 at various densities using a self-consistent method in the t-matrix formulation. Three different forms of the two-body potentials are used: the Lennard-Jones potential, the Beck potential, and the Frost-Musulin potential. The same method is also applied to solid molecular hydrogen using the Mason-Rice two-body potential. The present approach is similar to that used to study the crystallization of neutron matter,[11] so its application to solids, whose physical properties are well known, should give an indication of the correctness of this approach.

In Sec. II we outline the t-matrix approach and the resulting equations of motion. In Sec. III we describe the solutions of the equations of motion in terms of partial waves, while Sec. IV deals with the self-consistent determination of the single-particle wave functions. In Sec. V we present the results of the method applied to solid He^3 and H_2 along with the results of other authors. Numerical details are presented in the Appendixes.

II. t MATRIX AND EQUATIONS OF MOTION

An exhaustive discussion of the t-matrix approach can be found in the paper of Guyer and Zane.[7] The original Hamiltonian for N atoms,

$$H=\sum_{i=1}^{N} T_i+\frac{1}{2}\sum_{i\neq j}^{N} V_{ij}\,, \tag{1}$$

is formally separated into $H=H_0+H_1$, where

$$H_0=\sum_{i=1}^{N} T_i+\frac{1}{2}\sum_{i\neq j}^{N} W_{ij}\,, \quad H_1=\frac{1}{2}\sum_{i\neq j}^{N}(V_{ij}-W_{ij}). \tag{2}$$

T_i is the kinetic-energy operator and V_{ij} is the two-body potential. The Hamiltonian H_0 is supposed to be exactly solvable, leading to localized orbitals. Expanding W_{ij} around the lattice site and retaining only quadratic terms, the eigenfunctions of H_0 turn out to be made up of harmonic-oscillator wave functions of unknown frequency ω. For example, the ground-state eigenfunction Φ_0 $(1, \ldots, N)$ satisfies

$$H_0\Phi_0(1,\ldots,N)=E_0\Phi_0(1,\ldots,N), \tag{3}$$

where $\Phi_0(1, \ldots, N)$ is a product of single-particle wave functions of Gaussian form

$$\Phi_0(1,\ldots,N)=\prod_{i}^{N}\varphi(i)\,, \tag{4}$$

$$\varphi(i)=(\alpha^{3/2}/\pi^{3/4})\,e^{-\alpha^2(\vec{r}_i-\vec{R}_i)^2/2}\,,$$

$\vec{R}_i$ being the lattice site of particle i. The parameter $\alpha^{-1}=(\hbar/m\omega)^{1/2}$ represents the spread of φ around the lattice site.

The Rayleigh-Schrödinger perturbation expansion of the energy shift $\Delta E=E-E_0$ gives rise to the following expression:

$$E=\sum_i\langle T_i\rangle+\frac{1}{2}\sum_{i\neq j}\langle t_{ij}\rangle, \tag{5}$$

where the t matrix is defined as

$$t_{12}=V_{12}g/\langle g\rangle, \tag{6}$$

g being the correlation function defined as

$$\psi_{12}=\varphi(1)\varphi(2)g\,. \tag{7}$$

Here ψ_{12} is the two-body wave function, and angular brackets represent expectation values, i.e.,

$$\langle\cdots\rangle=\langle\Phi_0(1,\ldots,N)|\cdots|\,\Phi_0(1,\ldots,N)\rangle\,.$$

The Bethe-Goldstone equation in its full generality is too complicated to handle and hence Iwamoto and Namaizawa[9] and later Guyer and Zane[7] have employed a simplified version of it (hereafter referred to as the INGZ equation). The general equation has been studied in detail only in the context of nuclear matter. A full discussion of the work done on the solution of the equation for application to quantum crystals can be found in a review

paper by Brandow.[8] The INGZ equation reads

$$[T_1+T_2+U(1)+U(2)+V_{12}]\psi_{12}=E_{12}\psi_{12}, \tag{8}$$

where T_1 and T_2 are the kinetic-energy operators of particles 1 and 2, respectively, and $U(i)$ defined by

$$\varphi(i)U(i)\varphi(i)=\sum_{j=1}^{N}\frac{\int\varphi(i)\varphi(j)V_{ij}\psi_{ij}\,d\vec{r}_j}{\int\varphi(i)\varphi(j)\psi_{ij}d\vec{r}_i\,d\vec{r}_j} \tag{9}$$

is the self-consistent one-body potential, which in turn implies a knowledge of $\psi_{ij}(\vec{r}_{ij})$ itself. [Actually, Sarkissian and Guyer and Zane have incorporated some further terms which are not shown in Eq. (8); these terms arise from a choice of single-particle potential which differs somewhat from Eq. (9). Brandow has argued that the simple-form equations (8) and (9) should be more accurate than the modified form used by Guyer and co-workers.]

In their work, Guyer and co-workers choose $U(i)$ to be a harmonic-oscillator potential. One way to choose the frequency ω of this oscillator would be to treat this as a variational parameter, and adjust this to minimize the total energy. However, in the present work we have determined ω (which enters the wave function through the parameter α) in a self-consistent manner to be discussed in Sec. IV.

If we expand $U(i)$ in a Taylor series to second order,

$$U(i)=U(0)+\tfrac{1}{2}m\omega^2(\vec{r}_i-\vec{R}_i)^2, \tag{10}$$

and choose relative and "center-of-mass" coordinates $\vec{r}$ and $\vec{R}$, respectively, defined by

$$\vec{r}=\vec{r}_2-\vec{r}_1, \quad 2\vec{R}=\vec{r}_1+\vec{r}_2, \tag{11}$$

the Hamiltonian of Eq. (8) can be written

$$H(12)=H(R)+H(r), \tag{12}$$

where

$$\begin{aligned}H(R)&=-(\hbar^2/4m)\,\nabla_R^2+m\omega^2\,[R-\tfrac{1}{2}(R_1+R_2)]^2,\\ H(r)&=-(\hbar^2/m)\nabla_r^2+\tfrac{1}{4}m\omega^2(\vec{r}-\vec{\Delta})^2+2U(0)+V(r),\end{aligned} \tag{13}$$

$\vec{\Delta}\equiv\vec{R}_2-\vec{R}_1$ being the distance between particles 1 and 2. The eigenfunction ψ_{12} can, therefore, be written in the product form

$$\psi_{12}=\psi(\vec{r})\Phi(\vec{R}), \tag{14}$$

where

$$\Phi(\vec{R})=\frac{\alpha^{3/2}}{(\frac{1}{2}\pi)^{3/4}}\exp\{-\alpha^2[\vec{R}-\tfrac{1}{2}(\vec{R}_1+\vec{R}_2)]^2\} \tag{15}$$

and satisfies the eigenvalue equation

$$H(R)\psi(\vec{R})=\tfrac{3}{2}\hbar\omega\psi(\vec{R}). \tag{16}$$

The INGZ equation now reads

$$[-(\hbar^2/m)\nabla_r^2+\tfrac{1}{4}m\omega^2r^2-\tfrac{1}{2}m\omega^2\vec{r}\cdot\vec{\Delta}+V(\vec{r})]\psi(\vec{r})=E'_{12}\psi(\vec{r}), \tag{17}$$

where

$$E'_{12}=E_{12}-2U(0)-\tfrac{3}{2}\hbar\omega-\tfrac{1}{4}m\omega^2\Delta^2.$$

If $V=0$, the two-body wave function ψ_{ij} reduces to $\varphi(i)\varphi(j)$, which can be written

$$\varphi_{ij}\equiv\varphi(i)\varphi(j)=\varphi(\vec{r})\Phi(\vec{R}), \tag{18}$$

where

$$\varphi(\vec{r})=\frac{\alpha^{3/2}}{(2\pi)^{3/4}}\,e^{-\alpha^2(\vec{r}-\vec{\Delta})^2/4}. \tag{19}$$

III. SOLUTION OF TWO-BODY EQUATION

The term $\vec{r}\cdot\vec{\Delta}=r\Delta\cos\theta$ in Eq. (17) is a notable feature of the two-body Hamiltonian. It is clearly not invariant under space inversion, i.e., $H(\vec{r})\neq H(-\vec{r})$. This is highly reminiscent of the Stark effect. The $\cos\theta$ term has matrix elements different from zero only for states that differ by one unit in the angular momentum, i.e., $\langle l|\cos\theta\,|l'\rangle\propto\delta_l^{l'\pm1}$. In the previous treatments, the $\cos\theta$ term was set equal to unity, making Eq. (17) spherically symmetric. This is not strictly justified as one should, in principle, make a partial-wave expansion of $\psi(\vec{r})$ of the form

$$\psi(\vec{r})=\sum_{l=0}^{\infty}(2l+1)\psi_l(r)\,P_l(\cos\theta). \tag{20}$$

Upon substituting Eq. (20) into (17), multiplying

TABLE I. Contributions per particle to the potential energy for solid He^3 (bcc) from the first 15 shells using the Lennard-Jones potential at $\Omega=21$ cm^3/mole, $\alpha^2=1.24$ Å^{-2}. Kinetic energy = 14.94 °K; potential energy = −15.42 °K; $E/N=-0.48$ °K. Energies are in °K.

Shell No. k	N_k, No. of particles	Δ_k	ϵ_k, shell energy	$\frac{1}{2}N_k\epsilon_k$	U_k
1	8	3.564	−1.400	−5.598	−27.981
2	6	4.116	−1.766	−5.299	−14.611
3	12	5.820	−0.296	−1.774	−1.752
4	24	6.824	−0.110	−1.322	−0.650
5	8	7.129	−0.086	−0.345	−0.139
6	6	8.232	−0.039	−0.117	−0.023
7	24	8.969	−0.024	−0.286	−0.046
8	24	9.203	−0.021	−0.247	−0.023
9	24	10.080	−0.012	−0.145	−0.010
10	12	10.693	−0.008	−0.061	−0.003
11	12	11.640	−0.005	−0.031	−0.002
12	48	12.175	−0.004	−0.093	−0.004
13	30	12.348	−0.004	−0.054	−0.002
14	24	13.015	−0.003	−0.031	−0.001
15	24	13.496	−0.002	−0.026	−0.001

both sides by $P_l(\cos\theta)$, and integrating over θ, one obtains the following system of coupled differential equations for the various partial waves:

$$H_l''(x)+(\eta-E_l)H_l(x)+\frac{F(x)(-)^l}{2l+1}\times[(l+1)H_{l+1}(x)-lH_{l-1}(x)]=0,$$

$$l=0,1,2,3,\ldots \qquad (21)$$

with the following notation:

$$x=r/r_0, \quad d=\Delta/r_0,$$

$$\rho=m\gamma/r_0^3 \quad (\gamma=4, \text{ fcc}; \ \gamma=2, \text{ bcc}),$$

where ρ is the density, $a=\alpha r_0$,

$$H_l(x)=x\psi_l(x), \quad F(x)=\tfrac{1}{2}a^4xd,$$

$$E_l=\tfrac{1}{4}a^4x^2+\frac{mr_0^2}{\hbar^2}V(\vec{x})+\frac{l(l+1)}{x^2},$$

and

$$\eta=\frac{mr_0^2}{\hbar^2}E_{12}-\frac{2mr_0^2}{\hbar^2}U(0)-\tfrac{3}{2}a^2-\tfrac{1}{4}a^4d^2.$$

After Eq. (21) has been solved for the H_l's, the energy per particle can be obtained from Eq. (5) in the form

$$\frac{E}{N}=\tfrac{3}{4}\hbar\omega+\frac{1}{2}\sum_{i\neq j}\frac{\int\varphi(i)\varphi(j)V_{ij}\psi_{ij}\,d\vec{r}_i\,d\vec{r}_j}{\int\varphi(i)\varphi(j)\psi_{ij}\,d\vec{r}_i\,d\vec{r}_j}$$

$$=\tfrac{3}{4}\hbar\omega+\frac{1}{2}\sum_k N_k\epsilon_k. \qquad (22)$$

The first term on the right-hand side is just the kinetic energy per particle for a simple-harmonic-oscillator (SHO) potential. N_k is the number of particles in the kth shell and ϵ_k is the shell energy, i.e., the potential energy of an atom owing to its interaction with another atom in the kth shell. ϵ_k may be written in the form (Appendix A)

$$\epsilon_k=\frac{\int_0^\infty xe^{-a^2x^2/4}V(\vec{x})[\hat{j}_0(iy_k)H_0(x)+3\hat{j}_1(iy_k)H_1(x)+5\hat{j}_2(iy_k)H_2(x)+\cdots]dx}{\int_0^\infty xe^{-a^2x^2/4}[\hat{j}_0(iy_k)H_0(x)+3\hat{j}_1(iy_k)H_1(x)+5\hat{j}_2(iy_k)H_2(x)+\cdots]dx}. \qquad (23)$$

The various quantities are defined as follows:

$$y_k=-\tfrac{1}{2}a^2xd_k, \quad \Delta_k=r_0d_k.$$

Δ_k is the distance from the atom under consideration to the kth shell and $\hat{j}_n(ix)=j_n(ix)$ is the spherical Bessel function if n is even and $\hat{j}_n(ix)=ij_n(ix)$ if n is odd. $V(\vec{x})$ has been assumed to be the same for all waves. For a quantum mechanical system whose potentials depend on spin and angular momentum we must use a more general expansion than Eq. (20) by including a spin wave function χ_s^{Ms} on the right-hand side.

TABLE II. Contributions per particle to the potential energy for solid He^3 (bcc) from the first 15 shells using the Lennard-Jones potential $\Omega=23$ cm^3/mole, $\alpha^2=1.12$ Å^{-2}. Kinetic energy = 13.45 °K; potential energy = −14.38 °K; $E/N=-0.93$ °K. Energies are in °K.

Shell No. k	N_k, No. of particles	Δ_k	ϵ_k, shell energy	$\frac{1}{2}N_k\epsilon_k$	U_k
1	8	3.672	−1.140	−5.640	−26.228
2	6	4.242	−1.620	−4.860	−12.998
3	12	5.998	−0.255	−1.527	−1.613
4	24	7.033	−0.091	−1.098	−0.597
5	8	7.347	−0.071	−0.286	−0.125
6	6	8.484	−0.032	−0.097	−0.021
7	24	9.243	−0.020	−0.239	−0.036
8	24	9.485	−0.017	−0.206	−0.028
9	24	10.389	−0.010	−0.121	−0.012
10	12	11.021	−0.007	−0.043	−0.004
11	12	11.996	−0.004	−0.026	−0.002
12	48	12.548	−0.003	−0.079	−0.005
13	30	12.726	−0.003	−0.046	−0.003
14	24	13.413	−0.002	−0.027	−0.001
15	24	13.910	−0.002	−0.022	−0.001

IV. SELF-CONSISTENT APPROACH

Equations (21)–(23) could, in principle, be solved to give the ground-state energy per particle of a quantum solid with a given structure at a given density ρ if α $[\equiv(m\omega/\hbar)^{1/2}]$ is known at that density. In this paper we propose to determine α at a given density self-consistently, making full use of $U(0)$, the one-body potential at the lattice site. The method is as follows. We obtain an equation for α by eliminating $U(0)$ between the two following expressions:

$$U(0)=2\sqrt{2}\sum_k N_k\frac{\int_0^\infty e^{-3\alpha^2(\vec{r}-\vec{\Delta}_k)^2/4}V(\vec{r})\psi(\vec{r})\,d\vec{r}}{\int_0^\infty e^{-\alpha^2(\vec{r}-\vec{\Delta}_k)^2/4}\psi(\vec{r})\,d\vec{r}}, \qquad (24a)$$

$$U(0)=\sum_k N_k\epsilon_k-\tfrac{3}{4}\hbar\omega. \qquad (24b)$$

Equation (24a) is obtained by putting $\vec{r}_i=\vec{R}_i$ in the exact definition of $U(i)$, Eq. (9). Equation (24b)

is obtained from Eqs. (22) and (23) (see Appendix B). At the same time the knowledge of $\psi(\vec{r})$ allows one to evaluate ϵ_k from Eq. (22) and, consequently, $U(0)$ from Eq. (24b). The process is repeated for different α's until the two U's coincide to within 1%.

This method has been used previously by Sarkissian,[6] and the α^2 versus molar volume in the paper of Guyer and Zane[7] is obtained with this method.

V. RESULTS AND DISCUSSIONS

In order to solve for $\psi(\vec{r})$ exactly, we would have to solve a set of infinite coupled differential equations for the H_l's. However, if the present method is to be at all practical, there must exist an integer l_{max} such that the sum from $l=0$ to ∞ in Eq. (20) is well represented by the sum from $l=0$ to l_{max}. This reduces the number of differential equations to $(l_{max}+1)$.

A. Solid He^3

We began with the study of solid He^3 with a bcc structure and a specific two-body potential $V(\vec{r})$. Three different two-body potentials were used.

(a) Lennard-Jones potential

$$V(r)=40.8\,[(2.556/r)^{12}-(2.556/r)^{6}]; \tag{25}$$

(b) Frost-Musulin potential[12]

$$V(r)=\begin{cases}-12.54\left[1+8.01\left(1-\dfrac{2.98}{r}\right)\right]\exp\left[8.01\left(1-\dfrac{r}{2.98}\right)\right], & r<3.5\ \text{Å}\\ -7250\left(\dfrac{1.41}{r^6}+\dfrac{3.82}{r^8}\right), & r>3.5\ \text{Å};\end{cases} \tag{26}$$

(c) Beck potential[13]

$$V(r)=V_0\left[Ae^{-\alpha r-\beta r^6}-\frac{D}{(r^2+p^2)^3}\left(1+\frac{2.709+3p^2}{r^2+p^2}\right)\right], \tag{27}$$

where

$$V_0=10.371\ ^\circ\text{K},\quad A=44.62\times10^4,\quad \alpha=4.39\ \text{Å}^{-1},$$
$$D=972.5,\quad \beta=3.746\times10^{-4}\ \text{Å}^{-1},\quad p=0.675\ \text{Å}.$$

The above potentials are in °K, with r measured in Å. Several increasing values of l_{max} were chosen, and the resulting system of $(l_{max}+1)$-coupled differential equations solved numerically for the ground-state eigenfunctions. These solutions were then used in Eq. (23) to compute the shell energy ϵ_k for various shells at a fixed density. The recursion relation

$$[(2n+1)/z]j_n(z)=j_{n+1}(z)+j_{n-1}(z) \tag{28}$$

TABLE III. Contributions per particle to the potential energy for solid He^3 (bcc) from the first 15 shells using the Lennard-Jones potential at $\Omega=23.94$ cm^3/mole, $\alpha^2=1.05$ Å^{-2}. Kinetic energy = 12.63 °K; potential energy = −13.73 °K; $E/N=-1.10$ °K. Energies are in °K.

Shell No. k	N_k, No. of particles	Δ_k	ϵ_k, shell energy	$\frac{1}{2}N_k\epsilon_k$	U_k
1	8	3.724	−1.376	−5.503	−25.114
2	6	4.300	−1.544	−4.631	−12.418
3	12	6.080	−0.242	−1.450	−1.603
4	24	7.129	−0.084	−1.010	−1.010
5	8	7.448	−0.065	−0.262	−0.126
6	6	8.600	−0.029	−0.088	−0.021
7	24	9.370	−0.018	−0.218	−0.032
8	24	9.615	−0.016	−0.188	−0.029
9	24	10.531	−0.009	−0.111	−0.012
10	12	11.171	−0.007	−0.039	−0.004
11	12	12.160	−0.004	−0.024	−0.002
12	48	12.719	−0.003	−0.072	−0.005
13	30	12.900	−0.003	−0.041	−0.003
14	24	13.597	−0.002	−0.024	−0.001
15	24	14.100	−0.002	−0.020	−0.001

TABLE IV. Contributions per particle to the potential energy for solid He^3 (bcc) from the first 15 shells using the Frost-Musulin potential at $\Omega=21$ cm^3/mole, $\alpha^2=1.33$ Å^{-2}. Kinetic energy = 16.05 °K; potential energy = −14.38 °K; $E/N=1.67$ °K. Energies are in °K.

Shell No. k	N_k, No. of particles	Δ_k	ϵ_k, shell energy	$\frac{1}{2}N_k\epsilon_k$	U_k
1	8	3.564	−1.346	−5.386	−29.246
2	6	4.116	−1.683	−5.050	−13.578
3	12	5.820	−0.240	−1.439	−1.230
4	24	6.824	−0.095	−1.146	−0.471
5	8	7.129	−0.074	−0.296	−0.098
6	6	8.232	−0.034	−0.102	−0.018
7	24	8.969	−0.021	−0.254	−0.031
8	24	9.203	−0.018	−0.216	−0.024
9	24	10.080	−0.011	−0.128	−0.010
10	12	10.693	−0.008	−0.045	−0.003
11	12	11.640	−0.005	−0.028	−0.002
12	48	12.175	−0.003	−0.083	−0.004
13	30	12.348	−0.003	−0.048	−0.002
14	24	13.015	−0.002	−0.028	−0.001
15	24	13.496	−0.002	−0.023	−0.001

for the spherical Bessel functions was used. It was found that the shell energy in general increased with increasing l_{max} and saturated at $l_{max} \approx 20$. The value $l_{max} = 25$ was finally chosen for the computation. Several tests were made to ensure that the computer solutions generated the ground-state eigenfunctions for the set of equations (21). For example, the eigenfunctions were plotted to demonstrate that they were indeed nodeless. Another test is described in Appendix C.

With this problem out of the way, we proceeded as described in Sec. IV to determine the ground-state energy per particle for He^3 at several densities. The results are summarized in Tables I–VII. In each table, only the contributions of the first 15 shells are shown, although it was found that the first 20 shells were needed to make the sum in Eq. (22) converge, i.e., the contribution of the higher shells to the potential energy was much less than 0.1%. The columns labeled U_k give the shell contributions to $U(0)$, i.e.,

$$U(0) = \sum_k U_k ,$$

$$U_k = 2\sqrt{2}\, N_k \frac{\int e^{-3\alpha^2(\vec{r}-\vec{\Delta}_k)^2/4}\, V(\vec{r})\psi(\vec{r})\, d\vec{r}}{\int e^{-\alpha^2(\vec{r}-\vec{\Delta}_k)^2/4}\, \psi(\vec{r})\, d\vec{r}} . \tag{29}$$

The self-consistency requirement is that

$$\sum_k U_k = \sum_k N_k \epsilon_k - \tfrac{3}{4}\hbar\omega , \tag{30}$$

which we tried to fulfill to within 1% or so. In Fig. 1 we show the results of our E/N using the Lennard-Jones potential along with the results of Pandharipande,[14] Hansen and Levesque,[15] Ebner and Sung,[16] and the experimental result.[17] Ω is the molar volume and is related to the density ρ through the equation

$$\Omega = m N_A/\rho , \tag{31}$$

where N_A is the Avogadro number. In Fig. 2 we show our E/N using the Frost-Musulin and Beck potentials. In Fig. 3 the self-consistent values of α^2 in the present work are compared with those

TABLE V. Contributions per particle to the potential energy for solid He^3 (bcc) from the first 15 shells using the Frost-Musulin potential at $\Omega = 23$ cm^3/mole, $\alpha^2 = 1.22$ Å^{-2}. Kinetic energy = 14.07 °K; potential energy = −13.42 °K; $E/N = 0.65$ °K. Energies are in °K.

Shell No. k	N_k, No. of particles	Δ_k	ϵ_k, shell energy	$\frac{1}{2}N_k\epsilon_k$	U_k
1	8	3.672	−1.357	−5.428	−27.157
2	6	4.242	−1.544	−4.629	−12.302
3	12	5.998	−0.208	−1.250	−1.207
4	24	7.033	−0.079	−0.953	−0.468
5	8	7.347	−0.062	−0.246	−0.087
6	6	8.484	−0.031	−0.092	−0.002
7	24	9.243	−0.020	−0.240	−0.003
8	24	9.485	−0.015	−0.185	−0.022
9	24	10.389	−0.010	−0.124	−0.001
10	12	11.021	−0.006	−0.038	−0.003
11	12	11.996	−0.004	−0.024	−0.001
12	48	12.548	−0.003	−0.070	−0.004
13	30	12.726	−0.003	−0.040	−0.002
14	24	13.413	−0.002	−0.023	−0.001
15	24	13.910	−0.002	−0.019	−0.001

TABLE VI. Contributions per particle to the potential energy for solid He^3 (bcc) from the first 15 shells using the Beck potential at $\Omega = 21$ cm^3/mole, $\alpha^2 = 1.30$ Å^{-2}. Kinetic energy = 15.73 °K; potential energy = −16.04 °K; $E/N = -0.32$ °K. Energies are in °K.

Shell No. k	N_k, No. of particles	Δ_k	ϵ_k, shell energy	$\frac{1}{2}N_k\epsilon_k$	U_k
1	8	3.564	−1.494	−5.974	−29.710
2	6	4.116	−1.886	−5.658	−15.435
3	12	5.820	−0.287	−1.722	−1.532
4	24	6.824	−0.108	−1.299	−0.552
5	8	7.129	−0.083	−0.331	−0.113
6	6	8.232	−0.037	−0.110	−0.019
7	24	8.969	−0.023	−0.271	−0.034
8	24	9.203	−0.019	−0.229	−0.026
9	24	10.080	−0.011	−0.134	−0.011
10	12	10.693	−0.008	−0.047	−0.003
11	12	11.640	−0.005	−0.028	−0.002
12	48	12.175	−0.004	−0.085	−0.004
13	30	12.348	−0.003	−0.049	−0.002
14	24	13.015	−0.002	−0.028	−0.001
15	24	13.496	−0.002	−0.023	−0.001

TABLE VII. Contributions per particle to the potential energy for solid He^3 (bcc) from the first 15 shells using the Beck potential at $\Omega = 23$ cm^3/mole, $\alpha^2 = 1.16$ Å^{-2}. Kinetic energy = 13.94 °K; potential energy = −14.88 °K; $E/N = -0.94$ °K. Energies are in °K.

Shell No. k	N_k, No. of particles	Δ_k	ϵ_k, shell energy	$\frac{1}{2}N_k\epsilon_k$	U_k
1	8	3.672	−1.487	−5.947	−27.737
2	6	4.242	−1.716	−5.149	−13.810
3	12	5.998	−0.247	−1.481	−1.451
4	24	7.033	−0.090	−1.075	−0.532
5	8	7.347	−0.068	−0.272	−0.108
6	6	8.484	−0.038	−0.113	−0.024
7	24	9.243	−0.019	−0.225	−0.032
8	24	9.485	−0.016	−0.196	−0.025
9	24	10.389	−0.008	−0.111	−0.010
10	12	11.021	−0.007	−0.039	−0.003
11	12	11.996	−0.004	−0.023	−0.001
12	48	12.548	−0.003	−0.071	−0.004
13	30	12.726	−0.003	−0.039	−0.002
14	24	13.413	−0.002	−0.022	−0.001
15	24	13.910	−0.002	−0.019	−0.001

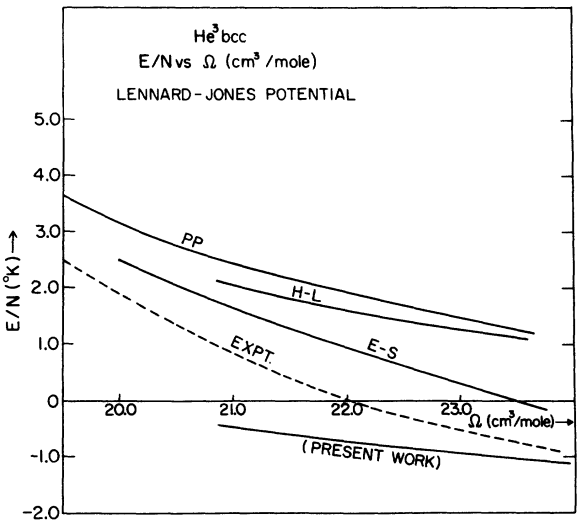

FIG. 1. Ground-state energy per particle of solid He^3 vs molar volume obtained from the present work compared with the results of Pandharipande (PP), Hansen and Levesque (H-L), Ebner and Sung (E-S), and the experimental results. All calculations used the Lennard-Jones potential.

computed in different ways by Guyer[18] and the previously mentioned authors.

The correlation function $g(\vec{r})$ defined by the equation

$$\psi(\vec{r}) = g(\vec{r})\varphi(\vec{r}) \tag{32}$$

should be zero at $r=0$ and should be well behaved as $r \to \infty$. For a more detailed discussion of $g(\vec{r})$, we refer the reader to Sarkissian's thesis, Sec. VIII of Ref. 8 and Appendix D. In the partial-wave method we will define

$$g_l(r) = \psi_l(r)/\varphi_l(r), \tag{33}$$

where $\varphi_l(r)$ is the lth component in the partial-wave expansion of $\varphi(\vec{r})$, i.e.,

$$\varphi(\vec{r}) = \sum_{l=0}^{\infty} (2l+1)\,\varphi_l(r) P_l(\cos\theta). \tag{34}$$

The specific form of $\varphi_l(r)$ is given in Eq. (A.8). $g_l(r)$ has been evaluated for $l=0, 1, 2, \ldots,$ 20 for different shells with the Lennard-Jones potential at $\Omega = 23.94$ cm^3/mole. The results for the first and fourth shells for $l=0$ to 7 are shown in Tables VIII and IX.

We can define an average correlation function

$$\bar{g} = (L+1)^{-1} \sum_{l=0}^{L} g_l(r). \tag{35}$$

Figure 4 shows plots of $\bar{g}$ for the first and fourth shells with L taken to be 20 again using the Lennard-Jones potential at a volume $\Omega = 23.94$ cm^3/mole. In Fig. 5 we show the corresponding correlation functions for the first shell obtained by Pandharipande, Ebner and Sung, and Hansen and Levesque.

An exact correlation function should always overshoot unity between $r=0$ and $r=\infty$ whatever the normalization of the wave functions. The normalization condition

$$\int \varphi(\vec{r})\psi(\vec{r})\, d\vec{r} = 1 \tag{36}$$

leads to

$$4\pi \sum_l \int_0^{\infty} g_l(r)\varphi_l^2(r) r^2\, dr = 1. \tag{37}$$

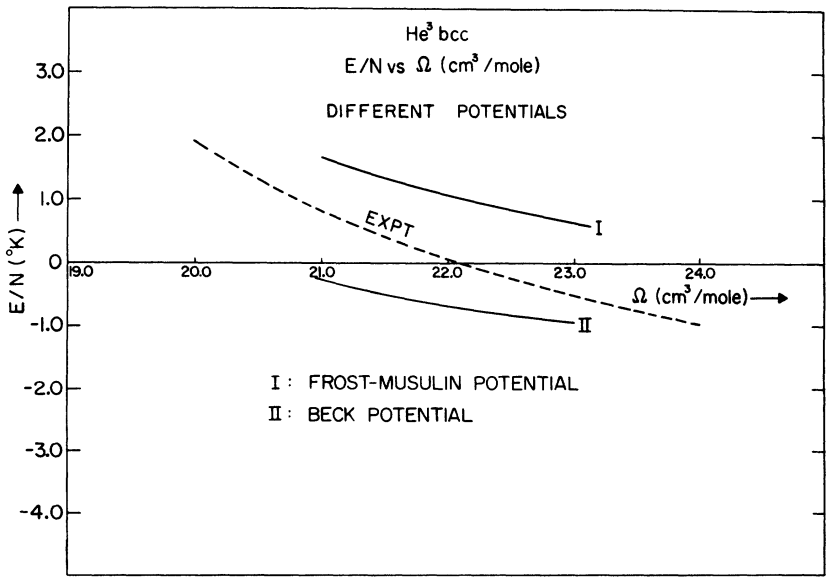

FIG. 2. Ground-state energy per particle of solid He^3 vs molar volume obtained using the Frost-Musulin (I) and Beck (II) potentials.

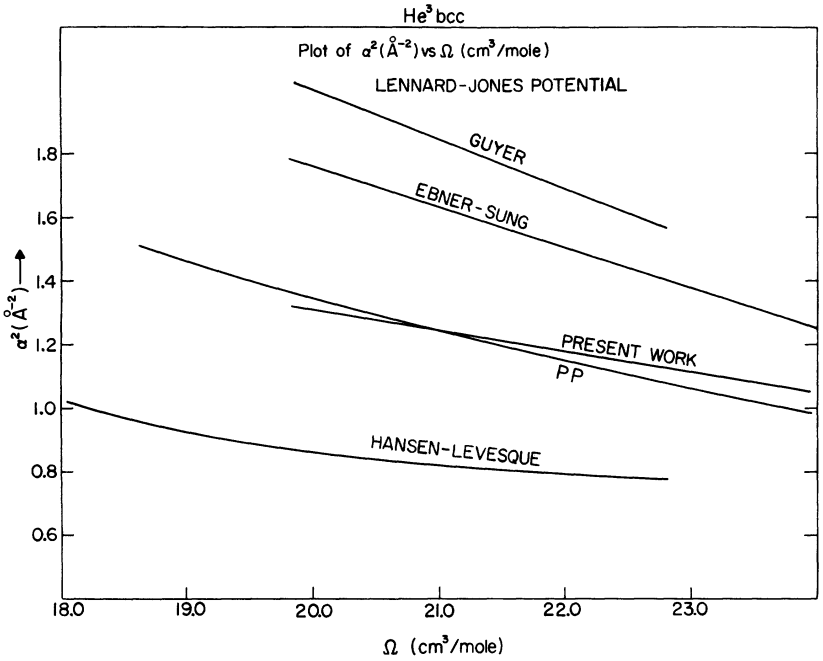

FIG. 3. $\alpha^2(\text{Å}^{-2})$ vs Ω obtained by different authors with the Lennard-Jones potential.

Since φ itself is normalized to unity and g obeys the condition $g=0$ at $r=0$ and $g\to 0$ as $r\to\infty$ (see Appendix D), g must be greater than unity at some finite r. The correlation functions of Pandharipande and Hansen and Levesque do not overshoot unity but approach it asymptotically. This means that their corresponding two-body wave functions will pick up less attractive energy than they should. (However, this could be compensated for by an increase in the kinetic energy.)

Another interesting quantity is the "wound integral" κ defined by Brandow[8]:

$$\kappa \approx \frac{N_1}{\Delta_1}\left(\frac{\alpha^2}{2\pi}\right)^{1/2}\int_0^\infty re^{-\alpha^2(r-\Delta_1)^2/2}\,h(r)\,dr, \quad (38)$$

where

$$h(r)\equiv[1-\bar{g}(r)]^2. \quad (39)$$

κ gives an indication of how good the two-body approximation is in this problem. The two-body approximation should be good if $\kappa \ll 1$. We have estimated κ to be 0.24 at $\Omega = 23.94$ cm^3/mole. Brandow[8] gets $\kappa = 0.16$, the difference being due to our smaller α^2. This small value of κ indicates that the three-body effects should be fairly small. One effect of the three-body energy (which we have not calculated) would probably be to increase the interaction energy, especially at the smaller molar volumes. This would result in a higher E/N and a steeper dependence of E/N on the molar volume. These effects would act in the right direction to improve the agreement with experiments, especially with the Lennard-Jones and Beck potentials. If the three-body energy were incorporated in the self-consistency condition for α, this should also increase the values of α somewhat.[8]

B. Solid H_2

The above method was applied to study the ground-state energy per particle for solid molec-

TABLE VIII. Correlation functions for the first eight partial waves at $\Omega = 23.94$ cm^3/mole using the Lennard-Jones potential for the first shell. He^3(bcc); Lennard-Jones potential: $\Omega = 23.94$ cm^3/mole, $k = 1$; g_l, correlation functions for different partial waves.

r (Å) \ l	0	1	2	3	4	5	6	7
1.72	0.01	0.01	0.01	0.01	0.01	0.02	0.02	0.03
2.06	0.15	0.16	0.19	0.22	0.27	0.32	0.38	0.44
2.41	0.50	0.52	0.57	0.64	0.71	0.79	0.86	0.93
2.75	0.79	0.82	0.86	0.91	0.97	1.03	1.08	1.12
3.27	1.00	1.01	1.03	1.06	1.09	1.12	1.13	1.15
3.61	1.04	1.05	1.06	1.08	1.10	1.11	1.12	1.12
3.96	1.05	1.06	1.07	1.08	2.09	1.09	1.10	1.10
4.13	1.05	1.06	1.06	1.07	1.08	1.08	1.09	1.08
4.47	1.05	1.05	1.05	1.06	1.06	1.06	1.06	1.06
4.82	1.04	1.04	1.04	1.04	1.05	1.05	1.05	1.04
5.16	1.03	1.03	1.03	1.03	1.03	1.03	1.03	1.03
5.50	1.02	1.02	1.02	1.02	1.02	1.02	1.02	1.01
5.68	1.01	1.01	1.01	1.01	1.01	1.01	1.01	1.01
5.85	1.01	1.01	1.01	1.01	1.01	1.00	1.00	1.00
6.02	1.00	1.00	1.00	1.00	1.00	1.00	1.00	1.00
6.19	1.00	1.00	1.00	1.00	1.00	0.99	0.99	0.99

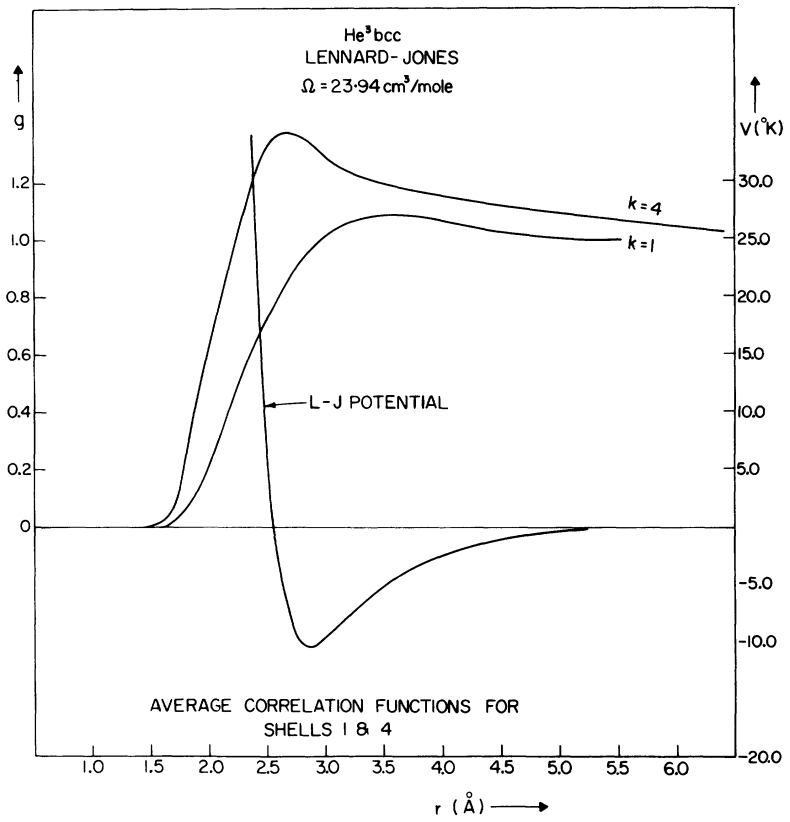

FIG. 4. Average correlation function $\bar{g}$ for the first and fourth shells using the Lennard-Jones potential at $\Omega = 23.94$ cm^3/mole.

ular hydrogen in the fcc structure. The two-body potential used was the Mason-Rice potential since that facilitated the comparison with the results of Østgaard[19]:

$$V(r) = 37.3\,[901\,953 \exp(-4.195/r) - 2416/r^6].$$

E/N for solid H_2 was computed at $\Omega = 20$ and 22 cm^3/mole and the results shown in Tables X and XI. The resulting E/N were found to be fairly insensitive to α since solid molecular hydrogen is not too quantum a solid. However, approximately 29 shells were required to ensure convergence of the potential energy. The experimental E/N for solid H_2 at $\Omega = 22$ cm^3/mole is -92 °K while the theoretical result is -85.1 °K. Østgaard[19] gets a corresponding value of -82 °K.

The results for solid He^3 show that E/N is rather sensitive to the two-body potential used. This is especially true since there is a very sensitive balance between the kinetic and potential energies. However, in the case of solid H_2, this problem is not as critical since the potential energy is quite different in magnitude from the kinetic energy.

ACKNOWLEDGMENTS

The authors would like to thank L. Nosanow and R. Guyer for informative discussions and B. Bran-

TABLE IX. Correlation functions for the first eight partial waves at $\Omega = 23.94$ cm^3/mole using the Lennard-Jones potential for the fourth shell. He^3(bcc); Lennard-Jones potential: $\Omega = 23.94$ cm^3/mole, $k = 4$; g_l, correlation functions for different partial waves.

r (Å) \ l	0	1	2	3	4	5	6	7
1.72	0.03	0.03	0.03	0.04	0.04	0.05	0.05	0.06
2.06	0.48	0.49	0.51	0.53	0.56	0.59	0.63	0.67
2.41	1.07	1.08	1.09	1.10	1.12	1.14	1.16	1.17
2.75	1.26	1.27	1.27	1.27	1.27	1.27	1.27	1.27
3.27	1.24	1.24	1.24	1.24	1.23	1.23	1.23	1.22
3.61	1.20	1.20	1.20	1.20	1.19	1.19	1.19	1.18
3.96	1.17	1.17	1.17	1.16	1.16	1.16	1.16	1.15
4.13	1.16	1.15	1.15	1.15	1.15	1.15	1.15	1.14
4.47	1.14	1.14	1.14	1.13	1.13	1.13	1.13	1.13
4.82	1.12	1.12	1.12	1.12	1.12	1.12	1.12	1.12
5.16	1.11	1.11	1.11	1.11	1.11	1.11	1.11	1.11
5.50	1.11	1.11	1.11	1.11	1.11	1.11	1.10	1.10
5.68	1.10	1.10	1.10	1.10	1.10	1.10	1.10	1.10
6.02	1.10	1.10	1.10	1.10	1.10	1.10	1.10	1.10
6.36	1.10	1.10	1.10	1.10	1.10	1.10	1.10	1.10
6.71	1.09	1.09	1.09	1.09	1.09	1.09	1.09	1.09

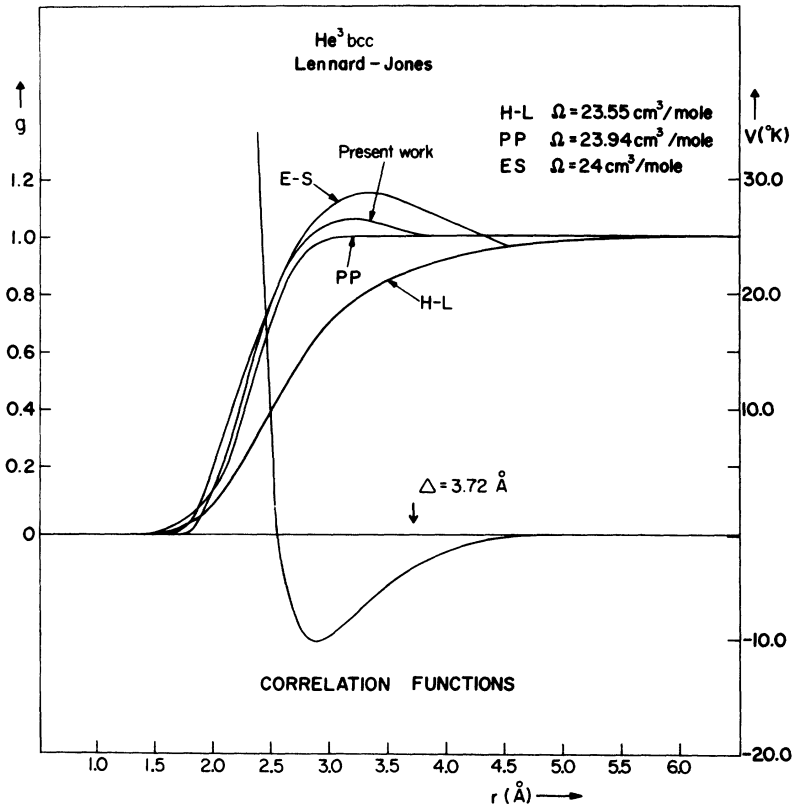

FIG. 5. Correlation function for the first shell compared with those of Pandharipande, Ebner and Sung, and Hansen and Levesque.

TABLE X. Contributions per particle to the potential energy for solid H_2 (fcc) from the first 15 shells using the Mason-Rice potential at $\Omega=20$ cm^3/mole, $\alpha^2=3.42$ Å^{-2}. Kinetic energy = 61.08 °K; potential energy = −144.0 °K; $E/N=-82.9$ °K. Energies are in °K.

Shell No. k	N_k, No. of particles	Δ_k	ϵ_k, shell energy	$\frac{1}{2}N_k\epsilon_k$	U_k
1	12	3.613	−14.61	−87.67	−272.0
2	6	5.110	−6.13	−18.38	−26.10
3	24	6.260	−1.73	−20.76	−27.50
4	12	7.226	−0.71	−4.25	−5.43
5	24	8.079	−0.36	−4.28	−5.33
6	8	8.851	−0.20	−0.82	−1.00
7	48	9.561	−0.13	−3.06	−3.69
8	6	10.220	−0.08	−0.25	−0.30
9	36	10.838	−0.06	−1.07	−1.26
10	24	11.426	−0.04	−0.51	−0.61
11	24	11.983	−0.03	−0.39	−0.45
12	24	12.514	−0.02	−0.30	−0.35
13	72	13.031	−0.02	−0.70	−0.81
14	48	13.996	−0.01	−0.34	
15	12	14.451	−0.01	−0.06	

TABLE XI. Contributions per particle to the potential energy for solid H_2 (fcc) from the first 15 shells using the Mason-Rice potential at $\Omega=22$ cm^3/mole, $\alpha^2=3.44$ Å^{-2}. Kinetic energy = 60.88 °K; potential energy = −146.0 °K; $E/N=-85.1$ °K. Energies are in °K.

Shell No. k	N_k, No. of particles	Δ_k	ϵ_k, shell energy	$\frac{1}{2}N_k\epsilon_k$	U_k
1	12	3.719	−16.48	−98.86	−267.0
2	6	5.260	−5.14	−15.41	−21.6
3	24	6.444	−1.45	−17.34	−22.8
4	12	7.438	−0.59	−3.56	−4.52
5	24	8.369	−0.30	−3.58	−4.44
6	8	9.110	−0.17	−0.68	−0.83
7	48	9.841	−0.11	−2.56	−3.08
8	6	10.520	−0.07	−0.21	−0.25
9	36	11.156	−0.04	−0.89	−2.50
10	24	11.761	−0.04	−0.43	
11	24	12.335	−0.03	−0.32	
12	24	12.882	−0.02	−0.25	
13	72	13.413	−0.02	−0.58	
14	48	14.407	−0.11	−0.25	
15	12	14.875	−0.01	−0.05	

dow for bringing to our attention the thesis of B. Sarkissian and for constant interest in our work. Two of us (S. M. C. and J. L.) wish to thank Dr. R. Jastrow for his hospitality at the Institute for Space Studies.

APPENDIX A

In this Appendix, we sketch the derivation of Eq. (23). The potential-energy term in Eq. (5) when written out explicitly takes the form

$$P=\frac{1}{2}\sum_{i\neq j}\frac{\int\int\varphi(i)\varphi(j)V_{ij}\psi_{ij}\,d\vec{r}_i\,d\vec{r}_j}{\int\int\varphi(i)\varphi(j)\psi_{ij}\,d\vec{r}_i\,d\vec{r}_j}. \tag{A1}$$

In terms of relative and center-of-mass coordinates $\vec{r}$ and $\vec{R}$, we can write

$$\varphi(i)\varphi(j)\equiv\Phi(\vec{R})\varphi(\vec{r}), \tag{A2}$$

where the normalized expressions for $\Phi(\vec{R})$ and $\varphi(\vec{r})$ are given by

$$\begin{aligned}\Phi(\vec{R})&=\frac{\alpha^{3/2}}{(\frac{1}{2}\pi)^{3/4}}\,e^{-\alpha^2[\vec{R}-\frac{1}{2}(\vec{R}_i+\vec{R}_j)]^2},\\ \varphi(\vec{r})&=\frac{\alpha^{3/2}}{(2\pi)^{3/4}}\,e^{-\alpha^2(\vec{r}-\vec{\Delta}_k)^2/4}.\end{aligned} \tag{A3}$$

Similarly, from Eqs. (14), (15), and (A3),

$$\psi_{ij}=\psi(\vec{r})\psi(\vec{R})=\psi(\vec{r})\Phi(\vec{R}). \tag{A4}$$

Therefore,

$$\frac{\int\int\varphi(i)\varphi(j)V_{ij}\psi_{ij}\,d\vec{r}_i\,d\vec{r}_j}{\int\int\varphi(i)\varphi(j)\psi_{ij}\,d\vec{r}_i\,d\vec{r}_j}=\frac{\int\int\varphi(\vec{R})\varphi(\vec{r})V(\vec{r})\Phi(\vec{R})\psi(\vec{r})\,d\vec{R}\,d\vec{r}}{\int\int\varphi(\vec{R})\varphi(\vec{r})\Phi(\vec{R})\psi(\vec{r})\,d\vec{R}\,d\vec{r}}. \tag{A5}$$

Furthermore, because of the normalization condition

$$\int\Phi^2(\vec{R})\,d\vec{R}=1, \tag{A6}$$

Eq. (A5) reduces to

$$\frac{\int\int\varphi(i)\varphi(j)V_{ij}\psi_{ij}\,d\vec{r}_i\,d\vec{r}_j}{\int\int\varphi(i)\varphi(j)\psi_{ij}\,d\vec{r}_i\,d\vec{r}_j}=\frac{\int\varphi(\vec{r})V(\vec{r})\psi(\vec{r})\,d\vec{r}}{\int\varphi(\vec{r})\psi(\vec{r})\,d\vec{r}}. \tag{A7}$$

We can expand $\varphi(\vec{r})$ in terms of partial waves similar to the expansion of $\psi(\vec{r})$ in Eq. (20):

$$\begin{aligned}\varphi(\vec{r})&=\frac{\alpha^{3/2}}{(2\pi)^{3/4}}\,e^{-\alpha^2(\vec{r}-\vec{\Delta}_k)^2/4}\\ &=\frac{\alpha^{3/2}}{(2\pi)^{3/4}}\,e^{-\alpha^2(r^2+\Delta_k^2)/4}\,e^{\alpha^2 r\Delta_k\cos\theta/2}\\ &=\frac{\alpha^{3/2}}{(2\pi)^{3/4}}\,e^{-\alpha^2(r^2+\Delta_k^2)/4}\\ &\quad\times\sum_{l=0}^{\infty}i^l(2l+1)j_l(iy_k)P_l(\cos\theta),\end{aligned} \tag{A8}$$

where $y_k=-\frac{1}{2}\alpha^2 r\Delta_k$. We have used the well-known expression

$$e^{ikr\cos\theta}=\sum_{l=0}^{\infty}i^l(2l+1)j_l(kr)P_l(\cos\theta). \tag{A9}$$

If we substitute Eqs. (A8) and (20) into (A7), and integrate over solid angles using the orthogonality properties of the Legendre polynomials, we get

$$\frac{\int\int\varphi(i)\varphi(j)V_{ij}\psi_{ij}\,d\vec{r}_i\,d\vec{r}_j}{\int\int\varphi(i)\varphi(j)\psi_{ij}\,d\vec{r}_i\,d\vec{r}_j}=\int_0^\infty xe^{-a^2x^2/4}V(x)\sum_{l=0}^{\infty}(2l+1)\hat{j}_l(iy_k)H_l(x)\,dx\Big/\int_0^\infty xe^{-a^2x^2/4}\sum_{l=0}^{\infty}(2l+1)\hat{j}_l(iy_k)H_l(x)\,dx \tag{A10}$$

in dimensionless variables. In terms of $\hat{j}_l$ and H_l, Eq. (A1) becomes

$$P=\frac{1}{2}\sum_k N_k\int_0^\infty xe^{-a^2x^2/4}V(x)\sum_{l=0}^{\infty}(2l+1)\hat{j}_l(iy_k)H_l(x)\,dx\Big/\int_0^\infty xe^{-a^2x^2/4}\sum_{l=0}^{\infty}(2l+1)\hat{j}_l(iy_k)H_l(x)\,dx$$

so that we obtain the expression for ϵ_k given in Eq. (23).

APPENDIX B

We write Eq. (9) in the form

$$\varphi(i)U(i)\varphi(i)=\sum_{j=1}^{N}\frac{A}{B}, \tag{B1}$$

where the numerator A is

$$A=\int\varphi(i)\varphi(j)V_{ij}\psi_{ij}\,d\vec{r}_j \tag{B2}$$

and the denominator B is

$$B=\int\int\varphi(i)\varphi(j)\psi_{ij}\,d\vec{r}_i\,d\vec{r}_j. \tag{B3}$$

Again, we write $\varphi(i)\varphi(j)=\Phi(\vec{R})\varphi(\vec{r})$ and

$\psi_{ij} = \Phi(\vec{R})\psi(\vec{r})$. A can then be written

$$A(\vec{\rho}_i) = \frac{\alpha^{9/2}}{(2\pi)^{3/4}(\frac{1}{2}\pi)^{3/2}} \int e^{-\alpha^2(2\vec{\rho}_i + \vec{r} - \vec{\Delta})^2/2} \times e^{\alpha^2(\vec{r} - \vec{\Delta})^2/4} V(r)\, d\vec{r}, \quad \text{(B4)}$$

where $\vec{\rho}_i \equiv \vec{r} - \vec{R}_i$. Similarly, B can be written

$$B = \int \Phi(\vec{R})\psi(\vec{R})\, d\vec{R} \int (\alpha^2/2\pi)^{3/4} e^{-\alpha^2(\vec{r} - \vec{\Delta}_k)^2/4} \psi(\vec{r})\, d\vec{r}$$

$$= (\alpha^2/2\pi)^{3/4} \int e^{-\alpha^2(\vec{r} - \vec{\Delta}_k)^2/4} \psi(\vec{r})\, d\vec{r} \quad \text{(B5)}$$

since Eq. (A6) holds.

Since $U(0)$ is the value of $U(i)$ evaluated at $\vec{r}_i = \vec{R}_i$, i.e., $\vec{\rho}_i = 0$, Eqs. (B1), (B4), and (B5) give

$$U(0) = 2\sqrt{2} \sum_k N_k \times \frac{\int e^{-3\alpha^2(\vec{r} - \vec{\Delta}_k)^2/4} V(\vec{r})\psi(\vec{r})\, d\vec{r}}{\int e^{-\alpha^2(\vec{r} - \vec{\Delta}_k)^2/4} \psi(\vec{r})\, d\vec{r}}. \quad \text{(B6)}$$

This expression can be written in terms of the H_l's and $\hat{j}_l$'s as follows:

$$U(0) = 2\sqrt{2} \sum_k N_k \int x e^{-3a^2(x^2 + d_k^2)/4} V(x) \sum_{l=0}^{\infty} (2l+1)\hat{j}_l(3iy_k) H_l(x)\, dx \Big/ \int x e^{-a^2(x^2 + d_k^2)/4} \sum_{l=0}^{\infty} (2l+1)\hat{j}_l(iy_k) H_l(x)\, dx. \quad \text{(B7)}$$

To obtain another equation for $U(0)$, we note that Eq. (5) can be written

$$E = \tfrac{3}{4}\hbar\omega + \frac{1}{2}\sum_i^N \int \varphi(i) U(i) \varphi(i)\, d\vec{r}. \quad \text{(B8)}$$

Using the expansion given by Eq. (10) we get

$$E/N = \tfrac{3}{4}\hbar\omega + \tfrac{1}{2}U(0) + \tfrac{1}{2}\int \varphi(i)[\tfrac{1}{2}m\omega^2(\vec{r}_i - \vec{R}_i)^2]\varphi(i)\, d\vec{r}_i,$$

$$E/N = \tfrac{3}{4}\hbar\omega + \tfrac{1}{2}U(0) + \tfrac{1}{2}(\tfrac{3}{4}\hbar\omega), \quad \text{(B9)}$$

$$E/N = \tfrac{9}{8}\hbar\omega + \tfrac{1}{2}U(0).$$

Since by definition

$$E/N = \tfrac{3}{4}\hbar\omega + \tfrac{1}{2}\sum_k N_k \epsilon_k, \quad \text{(B10)}$$

we can combine Eqs. (B9) and (B10) to obtain

$$U(0) = \sum_k N_k \epsilon_k - \tfrac{3}{4}\hbar\omega. \quad \text{(B11)}$$

APPENDIX C

If we take $V(\vec{r}) = 0$, the INGZ equation becomes [cf. Eq. (8)]

$$\{T_1 + T_2 + 2U(0) + \tfrac{1}{2}m\omega^2[(\vec{r}_1 - \vec{R}_1)^2 + (\vec{r}_2 - \vec{R}_2)^2]\}\varphi(1, 2) = E_{12}\varphi(1, 2), \quad \text{(C1)}$$

where E_{12} is a sum of SHO energies, i.e.,

$$E_{12} = E_1 + E_2 = 2[\tfrac{3}{2}\hbar\omega + U(0)]. \quad \text{(C2)}$$

In terms of relative coordinates, Eq. (C1) is [cf. Eq. (17)]

$$[-(\hbar^2/m)\nabla_r^2 + \tfrac{1}{4}m\omega^2(r^2 - 2\vec{r}\cdot\vec{\Delta})]\varphi(\vec{r}) = \eta_0\varphi(\vec{r}), \quad \text{(C3)}$$

where

$$\eta_0 = E_{12} - 2U(0) - \tfrac{3}{2}\hbar\omega - \tfrac{1}{4}m\omega^2\Delta^2. \quad \text{(C4)}$$

If we use Eq. (C2), η_0 becomes (in dimensionless units)

$$\eta_0 = (\tfrac{3}{2}a^2 - \tfrac{1}{4}a^4 d_k^2). \quad \text{(C5)}$$

Although η is not used directly in calculating the ground-state energies in this paper, Eq. (C5) does provide an independent check on the accuracy of the numerical solution of Eqs. (21) with $V(x) = 0$, and should also demonstrate the improved accuracy that is expected from using larger values of $l_{\max}$ in the partial-wave expansion of Eq. (20). Accordingly, Eqs. (21) have been solved for η_0 with different values of $l_{\max}$. In Fig. 6 we have plotted $\log_{10}|(\eta_0 - \eta_0^c)/\eta_0|$ vs $l_{\max}$ for the first, tenth, and fifteenth shell in a bcc lattice with $a = 4.4$. η_0 is given by Eq. (C5) and η_0^c is the corresponding numerical value. From these graphs we can conclude that (i) higher values of $l_{\max}$ are required to obtain a given accuracy as the shell numbers in-

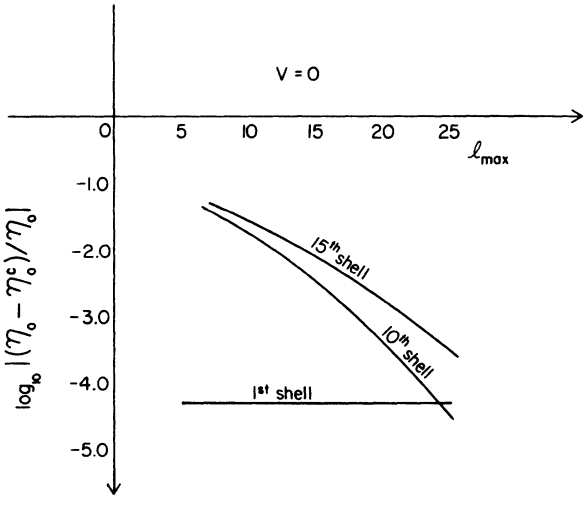

FIG. 6. $\mathrm{Log}_{10}|(\eta_0 - \eta_0^c)/\eta_0|$ vs $l_{\max}$ for the first, tenth, and fifteenth shell of a bcc structure.

crease and, (ii) $l_{max}=25$ gives an η_0^c that has a very small percentage difference compared to η_0 up to the fifteenth shell. In fact, we have found that $l_{max}=25$ is sufficient in the present work, as mentioned in Sec. V. Limits to the accuracy of the computer solution seem to depend only on the mesh size used in numerical integrations.

We present here a summary of the numerical method for the solution of the set of coupled equations in (21). We intend to obtain both the lowest eigenvalue and the corresponding eigenfunction. The approach is in two steps: first we reduce the problem to finding the solution to a set of linear equations which is also an eigenvalue problem for a matrix and second, we use numerical methods for finding the lowest eigenvalue of the matrix and the corresponding eigenvector.

For purposes of illustration, we consider the first three coupled equations in (21). If we apply central differences to the set of equations we have at the ith point

$$H_0^{i+1}-2H_0^i+H_0^{i-1}-k^2E_0^iH_0^i+k^2F^iH_1^i=-k^2\eta H_0^i,$$

$$H_1^{i+1}-2H_1^i+H_1^{i-1}-k^2E_1^iH_1^i+\tfrac{1}{3}k^2F^iH_0^i-\tfrac{2}{3}k^2F^iH_2^i=-k^2\eta H_1^i, \quad \text{(C6)}$$

$$H_2^{i+1}-2H_2^i+H_2^{i-1}-k^2E_2^iH_2^i-\tfrac{2}{5}k^2F^iH_1^i=-k^2\eta H_2^i,$$

where $1\leq i\leq(n-2)$ and n is the number of points in the mesh used. $k=x_{i+1}-x_i$ is constant and $H_l^i \equiv H_l(x_i)$, etc. $i=1$ is the point on the next-to-the-left endpoint and $i=(n-2)$ is the point on the next-to-the-right endpoint. At $i=1$, $H_l^{i-1}=0$ and at $i=(n-2)$, $H_l^{i+1}=0$ because of the boundary condition that each function vanishes at the endpoint.

Let us consider a vector $\vec{U}$ made up of blocks of elements where the ith block consists of the set (H_0^i, H_1^i, H_2^i). Then Eq. (C6) may be written as a matrix equation for all allowed values of i in the form

$$A\vec{U}=-k^2\eta\vec{U}, \quad \text{(C7)}$$

where

$$A=\begin{bmatrix} [K_1][I] & & & \\ [I][K_2][I] & & 0 & \\ & [I][K_3][I] & & \\ & & \ddots & \\ 0 & & & [I][K_n] \end{bmatrix}, \quad \text{(C8)}$$

$$\vec{U}=\begin{bmatrix} H_0^1 \\ H_1^1 \\ H_2^1 \\ \vdots \\ H_0^{n-2} \\ H_1^{n-2} \\ H_2^{n-2} \end{bmatrix}, \quad \text{(C9)}$$

$$I=\begin{bmatrix} 1 & 0 & 0 \\ 0 & 1 & 0 \\ 0 & 0 & 1 \end{bmatrix}, \quad \text{(C10)}$$

$$K_i=\begin{bmatrix} -2-k^2E_0^i & k^2F^i & 0 \\ \tfrac{1}{3}k^2F^i & -2-k^2E_1^i & -\tfrac{2}{3}k^2F^i \\ 0 & -\tfrac{2}{5}k^2F^i & -2-k^2E_2^i \end{bmatrix}. \quad \text{(C11)}$$

The formulation above can be generalized to any number of equations.

The solution of Eq. (C7) for the lowest eigenvalue and corresponding eigenvector is based on the power method. We assume that an *arbitrary* n-dimensional vector can be expanded in terms of the eigenvectors of a matrix, in this case the matrix A:

$$\vec{\chi}=\sum_{j=1}^{n}C_j\vec{U}_j. \quad \text{(C12)}$$

If we subtract a constant λ_0 times the identity matrix from A, take the inverse and multiply $\vec{\chi}$ on the left k times by $A-\lambda_0 I$, we get the series

$$\begin{aligned} (A-\lambda_0 I)^{-1}\vec{\chi}&=\sum_{j=1}^{n}\frac{C_j\vec{U}_j}{\lambda_j-\lambda_0}, \\ &\vdots \\ (A-\lambda_0 I)^{-k}\vec{\chi}&=\sum_{j=1}^{n}\frac{C_j\vec{U}_j}{(\lambda_j-\lambda_0)^k}, \end{aligned} \quad \text{(C13)}$$

where

$$A\vec{U}_n=\lambda_n\vec{U}_n. \quad \text{(C14)}$$

For sufficiently large values of k, the term with the eigenvalue closest to λ_0 will dominate the series in Eq. (C13) if we compare the absolute magnitudes of the terms. λ_0 is known as the shift. If λ_i is the smallest eigenvalue and $\lambda_0<\lambda_i$, the series con-

verges to

$$(A-\lambda_0 I)^{-k}\vec{\chi} = \frac{C_i \vec{U}_i}{(\lambda_i-\lambda_0)^k}, \tag{C15}$$

λ_i is then given by

$$\lambda_i = \lambda_0 + \frac{(A-\lambda_0 I)^{-k}\vec{\chi}}{(A-\lambda_0 I)^{-(k+1)}\vec{\chi}} \tag{C16}$$

and

$$\vec{U}_i \sim (A-\lambda_0 I)^{-k}\vec{\chi}. \tag{C17}$$

We know we have attained a sufficiently large value of k when Eq. (C16) gives a reasonably constant value of λ_i when k is increased further.

We have thus arrived at a method of obtaining the lowest eigenvalue and corresponding eigenfunction, which is: assume shifts λ_0 of decreasing sizes to find λ_i through Eq. (C16) in each case. If it yields the same eigenvalue each time, we may reasonably conclude that we have found the smallest eigenvalue.

In the present work, Eq. (C6) was replaced by a set of 26 equations, n was chosen to be 101, and $\vec{\chi}$, which has $26\times(n-2)=2574$ components, was chosen such that the first $26\times 26 = 676$ elements were each equal to zero and each of the remaining elements equal to 1.

APPENDIX D

In this Appendix, we will discuss some of the properties of the correlation function $g(\vec{r})$ defined in Eq. (32). If Eq. (32) is substituted into (17) we get the following equation of motion for $g(\vec{r})$:

$$\left(-\frac{\hbar^2}{m}\nabla_{\vec{r}}^2 + \frac{\hbar^2\alpha^2}{m}(\vec{r}-\vec{\Delta})\cdot\vec{\nabla}_r + V(\vec{r})\right) g(\vec{r}) = E^* g(\vec{r}), \tag{D1}$$

where

$$E^* \equiv E_{12} - 3\hbar\omega - 2U(0). \tag{D2}$$

Equation (19) has been used for $\varphi(\vec{r})$. In the limit $r\to\infty$, $V(\vec{r})\to 0$ and Eq. (D1) reduces to

$$-\frac{\hbar^2}{m}\frac{\partial^2 g(r)}{\partial r^2} + \frac{\hbar^2\alpha^2}{m} r \frac{\partial g(r)}{\partial r} = E^* g(r). \tag{D3}$$

TABLE XII. $\mathrm{Log}_{10}|(\eta_0-\eta_0^c)/\eta_0|$ vs $l_{\max}$ for He^3bcc at $\Omega=23.94$ cm^3/mole, using the Lennard-Jones potential: See Appendix D for details.

Shell no. k	δ
1	-8.0×10^{-2}
2	-9.6×10^{-2}
3	-1.9×10^{-2}
4	-7.6×10^{-3}
5	-6.0×10^{-3}
6	-2.6×10^{-3}
7	-1.7×10^{-3}
8	-1.5×10^{-3}
9	-8.0×10^{-4}
10	-3.0×10^{-4}

If we neglect the second-derivative term in Eq. (D3) for the moment and solve for $g(r)$, we obtain

$$g(r) \sim r^{\delta}, \tag{D4}$$

where

$$\delta \equiv E^*/(\hbar^2\alpha^2/m). \tag{D5}$$

In terms of dimensionless parameters, δ reduces to

$$\delta = \frac{\eta + \frac{1}{4}a^4d^2 - \frac{3}{2}a^2}{a^2} = \frac{\eta-\eta_0}{a^2}. \tag{D6}$$

Table XII shows shell numbers along with corresponding values of δ for He^3 at $\Omega=23.94$ cm^3/mole using the Lennard-Jones potential. We observe that δ is always negative and $|\delta|<<1$. These properties of δ are expected to hold for the other volumes.

If we insert (D4) into Eq. (D3) we obtain, for the second-derivative term,

$$\frac{\partial^2 g(r)}{\partial r^2} \sim \frac{|\delta|(|\delta|+1)}{r^{|\delta|+2}}. \tag{D7}$$

Since $|\delta|<<1$, we can indeed neglect the second-derivative term as $r\to\infty$.

*Also with the Dept. of Physics, City College of New York, New York, N.Y.
†National Academy of Sciences–National Research Council Resident Research Associate.
‡On leave of absence from the Tata Institute of Fundamental Research, Bombay, India.

[1]N. R. Werthamer, Am. J. Phys. **37**, 763 (1969).
[2]R. A. Guyer, in *Solid State Physics*, edited by F. Seitz, D. Turnbull, and H. Ehrenreich (Academic, New York, 1969), Vol. 23, p. 413.
[3]L. H. Nosanow, Phys. Rev. **146**, 120 (1966).
[4]N. G. Van Kampen, Physica (Utr.) **27**, 783 (1961).
[5]J. P. Hansen and E. L. Pollack, Phys. Rev. A **5**, 2051 (1972).
[6]B. Sarkissian, thesis (Duke University, 1968) (unpublished).
[7]R. A. Guyer and L. I. Zane, Phys. Rev. **188**, 445 (1969).
[8]B. H. Brandow, Ann. Phys. (N.Y.) **74**, 112 (1972).
[9]F. Iwamoto and H. Namaizawa, Prog. Theor. Phys. Suppl. 37 - 38, 234 (1966).
[10]K. A. Brueckner and J. Frohberg, Prog. Theor. Phys. Suppl. 33-35, 383 (1965).
[11]V. Canuto and S. M. Chitre, Phys. Rev. Lett. 30, 999 (1973).
[12]L. M. Bruch and I. J. McGee, J. Chem. Phys. **46**, 2959

(1967); J. Chem. Phys. **52**, 5884 (1970).
[13]D. E. Beck, Mol. Phys. **14**, 311 (1968).
[14]V. R. Pandharipande (private communication).
[15]J. P. Hansen and D. Levesque, Phys. Rev. **165**, 293 (1968).
[16]C. Ebner and C. C. Sung, Phys. Rev. A **4**, 269 (1971).
[17]R. C. Pandorff and D. O. Edwards, Phys. Rev. **169**, 222 (1968).
[18]R. A. Guyer, Solid State Commun. **7**, 315 (1969).
[19]E. Østgaard, J. Low Temp. Phys. **8**, 479 (1972).

PHYSICAL REVIEW A VOLUME 8, NUMBER 2 AUGUST 1973

Microscopic Theory of Rayleigh Scattering*

G. J. Gabriel
Department of Electrical Engineering and Radiation Research Laboratory, University of Notre Dame, Notre Dame, Indiana 46556
(Received 14 March 1972; revised manuscript received 24 August 1972).

A self-consistent, microscopic theory of scattering of light by molecular aggregates is evolved from the standpoints of random-phase-modulation theory and stochastic theory. Contemporary theory is founded on the premise that the scattered light spectrum is proportional to a four-dimensional Fourier transform of the molecular density-correlation function. This premise is justified only in a continuum representation of density, but it breaks down when the motion of discrete molecules is taken into account. The Rayleigh spectrum is shown to be a manifestation of translational degrees of freedom of molecules, much as the Raman spectrum is of internal degrees. Both the central and shifted components are attributed to propagating waves representing probability densities. Theoretical spectra are in agreement with experimental data in both the kinetic and hydrodynamic regimes, and the shifted frequencies are simply related to the rms speed of typical molecules. This theory also provides a mechanism which could account for deviations of total integrated intensity from that predicted by incoherent scattering. Such deviations are simply related to the ratio of intensities of the shifted and central components of the spectrum. Success of this theory, however, is not achieved without complete departure from conventional approaches of kinetic theory. By necessity, statistical aspects of the problem are approached through the use of a set of partial differential equations for the probability densities of continuous, differentiable stochastic processes. Statistical trajectories of molecules are characterized by a single function $h(\tau)$ defined as the logarithmic derivative of the conditional expectation value of velocity. Solutions based on the asymptotic behavior of $h(\tau)$ suggest the possibility for existence of other lines at the high-frequency end of the Rayleigh spectrum.

I. INTRODUCTION

The resurgence of interest in Rayleigh scattering of light in liquids and gases resulted to a large measure from invention of the laser and the analytical work of Komarov and Fisher,[1] who related the spectrum of scattered light to the function $S(\vec{K}, \omega)$, often called the structure factor, which is interpreted as a four-dimensional space-time Fourier transform of the molecular density-correlation function $G(\rho, \tau)$. It appeared possible, therefore, to infer some information on the dynamic structure of molecular aggregates through analysis of Rayleigh spectra.

In a series of papers, Yip and his co-workers[2-6] proposed a kinetic calculation of Rayleigh spectra by extension of developments in transport theory and neutron scattering. Almost concurrently, Mountain[7,8] developed a number of hydrodynamic calculations for the density-correlation function. It appears, however, that no attempt has been made at evolving a theory of light scattering from a unified set of principles. Although recent kinetic calculations of the spectra by Sugawara, Yip, and Sirovich[9,10]—based on approximate solutions of the Boltzmann transport equation for two specific interaction potentials—are in agreement with the observed spectra of Xe and CO_2 at a large viewing angle of 169.4°, they are not conclusive evidence that kinetic theory provides a truly microscopic theory of light scattering. Instead, these solutions essentially provide methods of calculation for the density-correlation function which, no doubt, are useful. As a theory of light scattering, however, composed of a self-consistent body of principles as a framework for interpreting observed phenomena, kinetic theory has neither explained the very existence of a Brillouin doublet as a manifestation of microscopic molecular events, nor predicted an analytical relation between the doublet frequencies and molecular quantities. In contrast, hydrodynamic theory interprets the doublet as a consequence of propagating density fluctuations and predicts the doublet frequencies in terms of acoustic velocity. To the extent that it attributes the observed phenomena to strictly collective or con-